PHILOSOPHICAL TRANSACTIONS OF THE ROYAL SOCIETY B

Phil. Trans. R. Soc. B (2012) **367**, 1245–1255
doi:10.1098/rstb.2011.0360

Research

Global oceanic production of nitrous oxide

Alina Freing†, Douglas W. R. Wallace‡ and Hermann W. Bange*

GEOMAR/Helmholtz Centre for Ocean Research Kiel, 24148 Kiel, Germany

We use transient time distributions calculated from tracer data together with *in situ* measurements of nitrous oxide (N_2O) to estimate the concentration of biologically produced N_2O and N_2O production rates in the ocean on a global scale. Our approach to estimate the N_2O production rates integrates the effects of potentially varying production and decomposition mechanisms along the transport path of a water mass. We estimate that the oceanic N_2O production is dominated by nitrification with a contribution of only approximately 7 per cent by denitrification. This indicates that previously used approaches have overestimated the contribution by denitrification. Shelf areas may account for only a negligible fraction of the global production; however, estuarine sources and coastal upwelling of N_2O are not taken into account in our study. The largest amount of subsurface N_2O is produced in the upper 500 m of the water column. The estimated global annual subsurface N_2O production ranges from 3.1 ± 0.9 to 3.4 ± 0.9 Tg N yr^{-1}. This is in agreement with estimates of the global N_2O emissions to the atmosphere and indicates that a N_2O source in the mixed layer is unlikely. The potential future development of the oceanic N_2O source in view of the ongoing changes of the ocean environment (deoxygenation, warming, eutrophication and acidification) is discussed.

Keywords: nitrous oxide; oceanic production; nitrification; denitrification

1. INTRODUCTION

Nitrous oxide (N_2O) is an atmospheric trace gas which influences the Earth's climate both directly and indirectly [1,2]: (i) In the troposphere, it acts as a strong greenhouse gas and (ii) owning to a relatively long atmospheric lifetime, N_2O can reach up to the stratosphere, where it acts as the major source for ozone-depleting nitric oxide radicals. Since the industrial revolution, the concentration of N_2O in the atmosphere has increased rapidly by about 18 per cent [3]. The dominant natural sources are believed to be soils and oceans, whereas anthropogenic sources mostly result from agricultural and industrial activities. N_2O is biologically produced in the ocean, and the resulting N_2O emissions play a major role for the atmospheric N_2O budget [4,5]. According to the Fourth Assessment Report of the Intergovernmental Panel on Climate Change, open ocean and coastal areas make up approximately 21 per cent and approximately 10 per cent of the total source of atmospheric N_2O of 17.7 Tg N yr^{-1}, respectively [5].

N_2O is microbially produced via nitrification ($NH_4^+ \rightarrow NO_2^- \rightarrow NO_3^-$) and denitrification ($NO_3^- \rightarrow NO_2^- \rightarrow N_2O \rightarrow N_2$). They are widely accepted to be the main production mechanisms of N_2O in the ocean [6]. N_2O can occur as a by-product during nitrification and as an intermediate during denitrification. However, the exact metabolism used for N_2O production during nitrification, the net behaviour of denitrification and their respective contributions to the global N_2O inventory in the ocean remain unclear [6–9].

Here, we present an estimate of the N_2O subsurface production rates by using the transient time distribution (TTD) approach. The discrepancy between the predicted global N_2O production and ocean–atmosphere flux estimates and its potential reasons as well as implications are discussed.

2. METHODS

In Freing *et al.* [10], TTDs calculated from tracer data together with *in situ* measurements of N_2O were used to estimate the concentration of biologically produced N_2O and N_2O production rates in the central North Atlantic Ocean. This approach to estimate N_2O production rates integrates the effects of potentially varying production/decomposition mechanisms along the transport path of a water mass. A new parametrization of N_2O production during nitrification depending linearly on the apparent oxygen utilization (AOU) and exponentially on temperature/depth was developed by Freing *et al.* [10], which is used here together with global gridded World Ocean Atlas (WOA) temperature [11], salinity [12] and oxygen [13] data and global gridded CFC-12 (i.e. dichlorodifluoromethane, CF_2Cl_2) data from the Global Data Analysis Project (GLODAP) [14] to calculate the global annual subsurface N_2O yield. We calculated a TTD age distribution and a mean age for every grid point. Because CFC-12 concentrations in the deep Pacific are too low to allow calculation of TTDs and the highest calculated mean age is 731 years, the mean age for every grid point

* Author for correspondence (hbange@geomar.de).
† Present address: NeuroCure Clinical Research Center, Charité-Universitätsmedizin Berlin, Berlin, Germany.
‡ Present address: Oceanography Department, Dalhousie University, Halifax, Nova Scotia, Canada.

One contribution of 12 to a Theo Murphy Meeting Issue 'Nitrous oxide: the forgotten greenhouse gas'.

with such a low CFC-12 concentration was set to 800 years. This choice results in a realistically smooth age distribution and is in line with the results of Matsumoto [15], who, using ^{14}C, found the deep ocean to be characterized by centennial rather than millennial timescales.

In order to estimate the background N_2O signal (N_2O_{eq}) in the ocean from the TTD, we need to know the time-dependent history of atmospheric concentrations. We used a synthesis of ice-core and firn data [16,17] merged with more recent air measurements. The data are available at http://daac.ornl.gov [18]. We assume a constant atmospheric mixing ratio of N_2O of 275 ppb prior to year 1800 and used a polynomial fit of the data from 1800 to the present day. For details on the atmospheric history of N_2O used and the use of TTDs to calculate $[N_2O]_{eq}$, see Freing *et al.* [10].

(a) *Open ocean apparent nitrous oxide production rate*

The bottom depth at each grid point was determined by using the 60 s resolution Earth Topography Digital Dataset (ETOPO) global elevation map distributed with the FERRET program (information is available at http://ferret.pmel.noaa.gov/Ferret/). A grid point was defined as an open ocean grid point if its bottom depth was more than 200 m. An apparent N_2O production rate for open ocean grid points was calculated in two ways (N_2OPR_{depth} and N_2OPR_{temp}) using the parametrizations developed by Freing *et al.* [10]. An apparent N_2O production rate depending on an apparent oxygen utilization rate (AOUR) and depth was calculated as

$$N_2OPR_{depth} = AOUR\, a_1 \exp\left(\frac{-z}{z_{sc}}\right) + a_2, \qquad (2.1)$$

where the coefficient values for the best fit are $a_1 = 0.0658$, $a_2 = -0.0065$, $z_{sc} = 20\,000$, z denotes the depth and AOUR = [AOU]/t, where t is the mean age of the water parcel calculated using the TTD method. An apparent N_2O production rate depending on AOUR and temperature was calculated as

$$N_2OPR_{temp} = AOUR\, a_1 \exp\left(\frac{-T}{T_{sc}}\right) + a_2, \qquad (2.2)$$

where the coefficient values for the best fit are $a_1 = 0.0665$, $a_2 = -0.0032$, $T_{sc} = 20\,000$, T denotes the temperature and AOUR = [AOU]/t, where t is the mean age of the water parcel calculated using the TTD method.

To exclude any undue influence of short-term seasonal variations affecting the near-surface ocean in the estimates, all production rates were calculated only for grid fields below the mixed layer. The mixed layer depth was determined by using the mixed layer climatology of de Boyer Montégut *et al.* [19]. The mixed layer depth is determined by an absolute change in temperature of 0.2°C compared with the temperature at 10 m depth. This parametrization accounts only for N_2O production by nitrification.

There are no CFC-12 data, and thus there is no mean age information available for the Arctic Ocean in the GLODAP dataset. A N_2OPR for the Arctic Ocean (N_2OPR_{arctic}) was estimated using the 25 per cent-quantile of the overall N_2OPR. This takes into account that, in general, the relevant biological productivity is comparatively low in the Arctic Ocean.

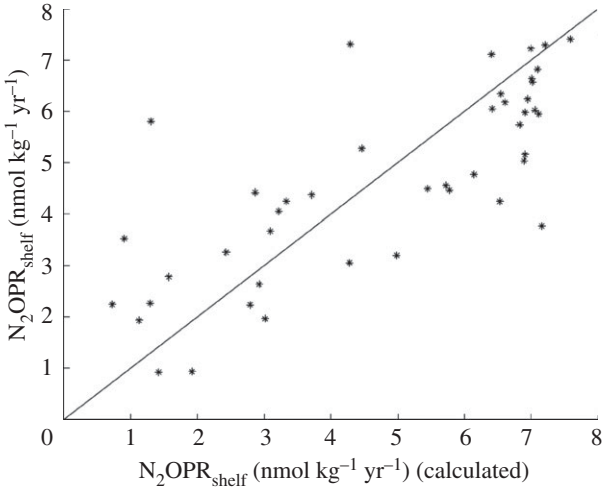

Figure 1. Shelf nitrous oxide (N_2O) production rates (nmol kg^{-1} yr^{-1}) calculated from N_2O data versus shelf N_2O production rates (nmol kg^{-1} yr^{-1}) calculated using equation (2.3).

(b) *Apparent nitrous oxide production rate on the continental shelves*

A grid point was defined as a shelf grid point if its bottom depth was 200 m or less. An apparent shelf N_2O production rate (N_2OPR_{shelf}) was calculated using 52 shelf data points from the N_2O database MEMENTO (version March 2009; see https://memento.ifm-geomar.de/) [20]. Unlike for N_2OPR, there is a good correlation between N_2OPR_{shelf}/AOUR and depth but not between N_2OPR_{shelf}/AOUR and temperature. Therefore, N_2OPR_{shelf} was estimated as

$$N_2OPR_{shelf} = AOUR\, a_1 \exp\left(\frac{-z}{z_{sc}}\right) + a_2, \qquad (2.3)$$

where the coefficient values for the best fit are $a_1 = 0.1795$, $a_2 = 0.5374$, $z_{sc} = 350$ and z denotes the depth. This parametrization accounts only for N_2O production by nitrification. The goodness of fit is illustrated in figure 1. Owing to lack of data, we did not attempt to calculate a production rate for the shelf of the Arctic Ocean.

(c) *Denitrification*

Denitrification can either produce or consume N_2O, depending on the surrounding conditions: it produces N_2O at the interface between suboxic and anoxic waters, while it consumes N_2O under (close to) anoxic conditions when the complete process of denitrification is performed [6,21].

To estimate production owing to denitrification, we used the collection of N_2O depth profiles archived in MEMENTO (version March 2009; figure 2) to determine the maximal and mean N_2O ($[N_2O^{omz}_{max}]$ and $[N_2O^{omz}_{mean}]$) concentration per depth and oxygen minimum zone. Following Codispoti *et al.* [22]

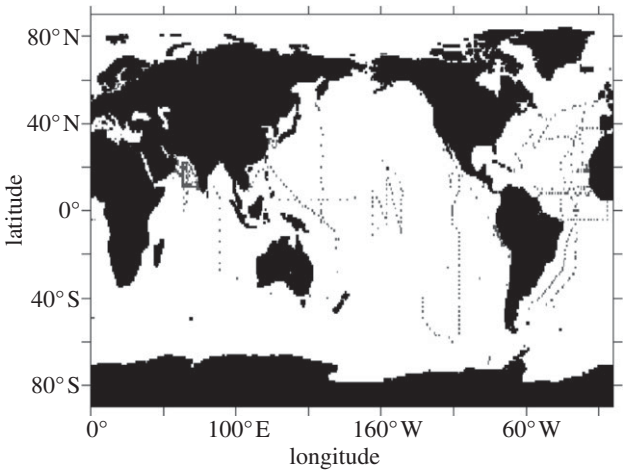

Figure 2. Available nitrous oxide depth profiles extracted from the MEMENTO database, version March 2009 [20].

and Stramma *et al.* [23], we defined suboxic zones as WOA fields with an oxygen content of less than 10 μmol kg^{-1}. This results in three main oxygen minimum zones, in the Arabian Sea, the Eastern Tropical North Pacific and the Eastern Tropical South Pacific, which is in good agreement with Paulmier *et al.* [24]. The difference between $[N_2O^{omz}_{max}]$ and $[N_2O^{omz}_{mean}]$ as well as the difference between $[N_2O^{omz}_{max}]$ and the estimated $[N_2O]$ ($= N_2OPR \times t + [N_2O]_{eq}$) resulting from nitrification were used as an estimate of the total amount of N_2O produced by denitrification. When $([N_2O^{omz}_{max}] - [N_2O])$ resulted in no N_2O production via denitrification, $[N_2O^{omz}_{mean}]$ and $[N_2O^{omz}_{max}]$ were used as a lower and upper boundary, respectively, for the total amount of N_2O produced via denitrification. The N_2O production rate owing to denitrification (N_2OPR^{denit}) was then calculated as

$$N_2OPR^{denit} = \frac{1}{t_{omz}}(([N_2O^{omz}_{max}] - (N_2OPR\,t + [N_2O]_{eq})) - \frac{1}{2}([N_2O^{omz}_{max}] - [N_2O^{omz}_{mean}])), \quad (2.4)$$

where t_{omz} is the average time a water parcel has already spent in the respective oxygen minimum zone [25–27] (table 1).

To estimate consumption owing to denitrification, we used the same collection of N_2O depth profiles (figure 2) to determine the minimal and mean N_2O ($[N_2O^{omz}_{min}]$ and $[N_2O^{omz}_{mean}]$) concentration per depth and oxygen minimum zone. We used an oxygen content of 4 μmol kg^{-1} as a threshold for an environment supporting a denitrification sink of N_2O, which marks out parts of the oxygen minimum zones described above. The difference between the estimated $[N_2O]$ resulting from nitrification and $[N_2O^{omz}_{min}]$, and the difference between $[N_2O^{omz}_{mean}]$ and $[N_2O^{omz}_{min}]$ were used as an estimate of the total amount of N_2O consumed by denitrification. When $([N_2O] - [N_2O^{omz}_{min}])$ resulted in no N_2O consumption via denitrification, $[N_2O^{omz}_{min}]$ and $[N_2O^{omz}_{mean}]$ were used as an upper and lower boundary, respectively, for the total amount of N_2O consumed by denitrification. The N_2O consumption rate owing to denitrification (N_2OCR^{denit}) was then calculated as

$$N_2OCR^{denit} = \frac{1}{t_{omz}}(((N_2OPR\,t + [N_2O]_{eq}) - [N_2O^{omz}_{min}]) - \frac{1}{2}([N_2O^{omz}_{mean}] - [N_2O^{omz}_{min}])). \quad (2.5)$$

Concentration differences in equation (2.5) indicating production were discarded for the purpose of this calculation.

Table 1. Average time of residence (years) per oxygen minimum zone (see text for details and references).

zone	average oxygen age
Arabian Sea	5
ETNP[a]	60
ETSP[a]	5

[a]ETNP and ETSP stand for eastern tropical North Pacific and eastern tropical South Pacific, respectively.

(d) *Integrated production estimates*

To estimate annual production rates per square metre, the respective N_2OPR was integrated over the water column. To estimate the magnitude of the global annual production of N_2O, firstly the volume of each grid cell was determined by integrating over the three dimensions: latitude, longitude and depth. The calculated volume was then multiplied by the respective N_2OPR to calculate the annual N_2O yield per grid cell. The sum of the annual N_2O yield of all ocean grid cells was used to estimate the global annual N_2O production. The integrated volume of a grid cell V_{gc} in cubic metres used in our calculations can be described as

$$V_{gc} = \frac{(\varphi_2 - \varphi_1)}{3}((R_{earth} - D_1)^3 - (R_{earth} - D_2)^3) \times (\sin(\Theta_2) - \sin(\Theta_1)), \quad (2.6)$$

where φ_1, φ_2 and Θ_1, Θ_2, with $\Theta_2 > \Theta_1$, are the longitudinal and latitudinal boundaries, respectively, of the respective grid cell in degrees, D_1, D_2, with $D_2 > D_1$, are the depth boundaries of the respective grid cell in metres and R_{earth} is the radius of the Earth in metres.

(e) *Nitrous oxide concentration*

$[N_2O]$ was predicted as

$$[N_2O] = [N_2O]_{eq} + N_2OPR\,t + f([O_2])\,N_2OPR^{denit}\,t_{omz} - g([O_2])N_2OCR^{denit}\,t_{omz}, \quad (2.7)$$

where f and g are switch functions, which determine whether denitrification contributes to $[N_2O]$. They are defined as

$$f([O_2]) = 1 \text{ for } [O_2] < 10\,\text{nmol}\,kg^{-1}; \quad f([O_2]) = 0 \text{ for } [O_2] \geq 10\,\text{nmol}\,kg^{-1} \quad (2.8)$$

and

$$g([O_2]) = 1 \text{ for } [O_2] < 4\,\text{nmol}\,kg^{-1}; \quad g([O_2]) = 0 \text{ for } [O_2] \geq 4\,\text{nmol}\,kg^{-1}. \quad (2.9)$$

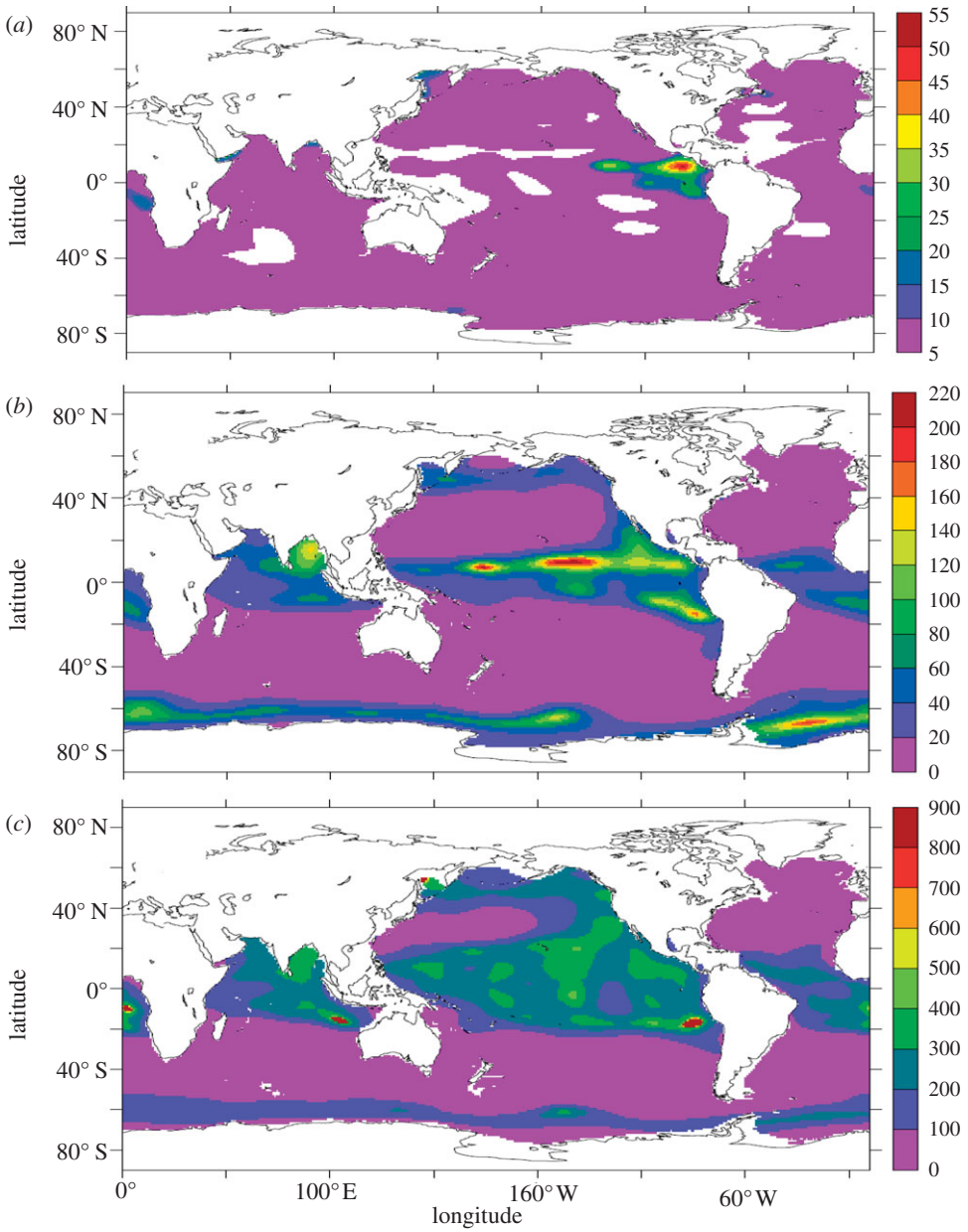

Figure 3. Global transient time distribution mean age (in years) in (*a*) 75 m, (*b*) 250 m and (*c*) 700 m.

N_2OPR is calculated as N_2OPR_{depth} or N_2OPR_{temp} according to equation (2.1) or (2.2), respectively.

(f) *Error estimates*

The predicted AOUR varied between 0.01 and 49 $\mu mol\ kg^{-1}\ yr^{-1}$, with an overall mean AOUR of $2.9 \pm 0.5\ \mu mol\ kg^{-1}\ yr^{-1}$ (1σ). These values are in good agreement with measurements [28,29]. This suggests that the use of a TTD-based mean age for rate calculations yields reliable rate estimates. Additionally, Tanhua *et al.* [30] found TTD-based estimates of anthropogenic carbon concentrations to be in good agreement with independent methods, suggesting the use of CFC-12 as tracers is a reliable basis for water mass age and hence estimation of background concentrations such as $[N_2O]_{eq}$.

In figure 3, the global TTD mean age in different water depths is shown. The TTD-derived mean ages presented here are in agreement with measurements of other tracers and model results [31,32].

The CFC-12, AOU and temperature measurements originate neither from the same water mass nor necessarily even from roughly the same time. Additionally, they represent some kind of average over latitude, longitude and depth. This is likely to dominate the error in our estimates. To estimate this error, we used 5900 open ocean data points below the mixed layer and 46 shelf data points below the mixed layer from our database. Using the gridded CFC concentrations from GLODAP, we calculated the difference between the original $[N_2O]$ and $[N_2O]_{est}$ with

$$[N_2O]_{est} = [N_2O]_{eq} + t\,N_2OPR, \tag{2.10}$$

where t is the mean age. The mean and median of the absolute percental differences can be found in table 2. It seems reasonable to use the median as a few very different data points can unduly influence the mean. It is likely that peculiar local conditions can lead to a

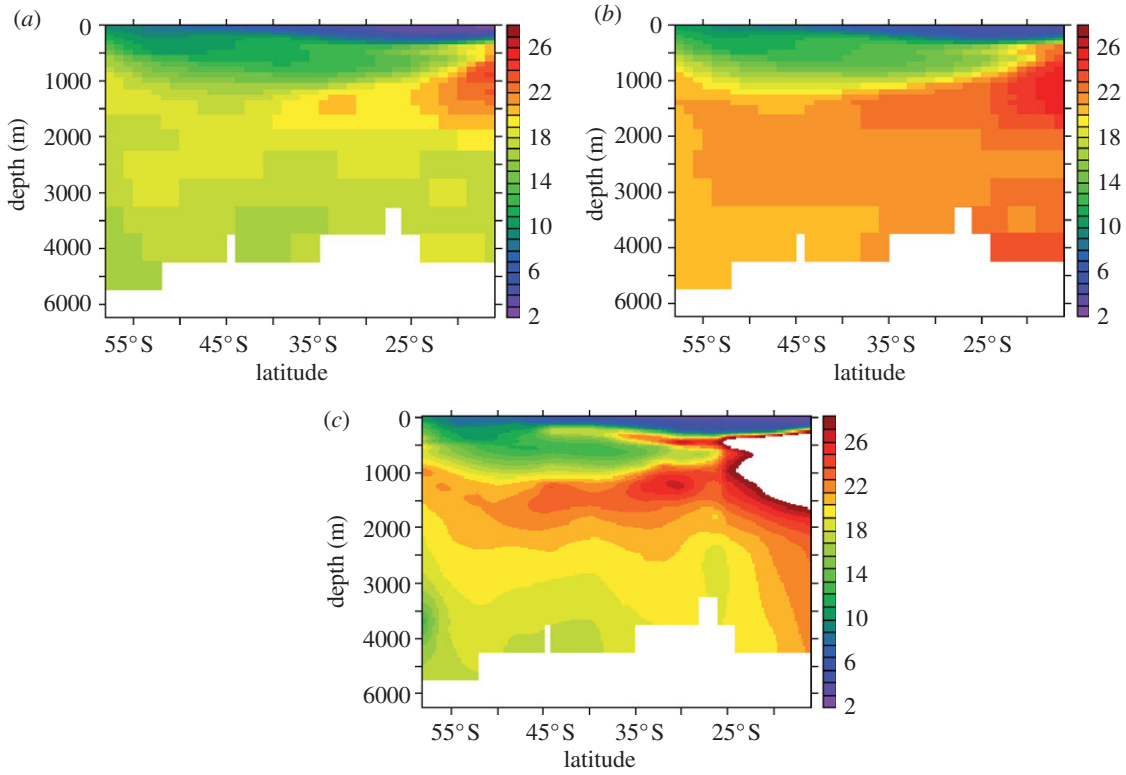

Figure 4. Section along 110° W (averaged between 100° W and 120° W). (*a*) Predicted [N_2O] (nmol kg^{-1}) according to N_2OPR_{depth}. (*b*) Predicted [N_2O] (nmol kg^{-1}) according to N_2OPR_{temp}. (*c*) Measured [N_2O] (nmol kg^{-1}) from Nevison *et al.* [33] and Farías *et al.* [34].

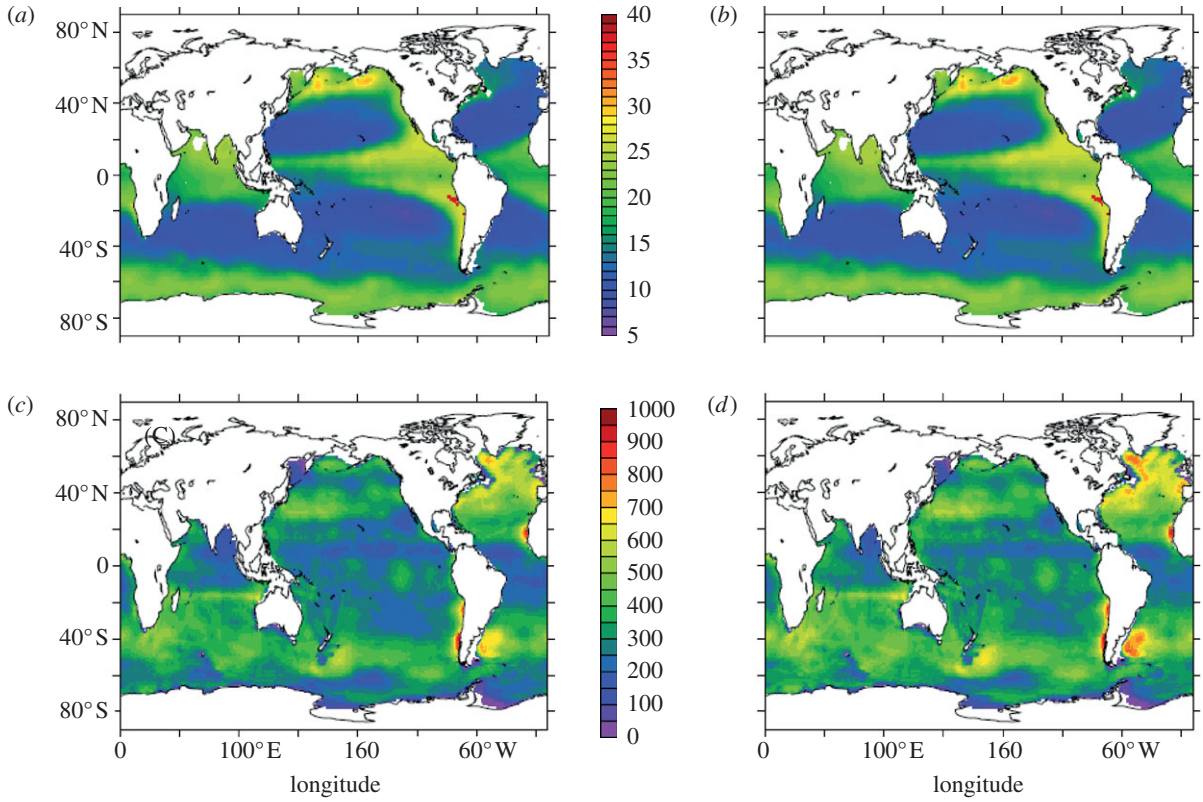

Figure 5. Global [N_2O] (nmol kg^{-1}) distribution in 200 m depth estimated using equations (2.7) with N_2OPR_{depth} (*a*) and equation (2.7) using N_2OPR_{temp} (*b*). (*a*,*b*) White areas in the Arabian Sea represent concentrations exceeding 40 nmol kg^{-1}. Annual N_2O production (μmol m^{-2} yr^{-1}) via nitrification integrated over the water column estimated using (*c*) equation (2.1) and (*d*) equation (2.2).

Table 2. Average percental error in concentration estimates (see text for details).

parameter	median (%)	mean (%)
N_2OPR_{depth}	24	34
N_2OPR_{temp}	22	34
N_2OPR_{shelf}	42	54

considerable misfit but this does not adequately represent the overall goodness of fit. As the mean age is crucial for both terms in equation (2.10), we assume that both terms contribute to the overall percental error in the same way. Table 2 suggests that the parametrization based on temperature (see equation (2.2)) seems to do a slightly better job. The amount of N_2O produced (consumed) by denitrification is estimated in a completely different fashion compared to nitrification rates (see §2*c*). Using the mean $[N_2O]$ from our database, the fraction of denitrification with regard to total annual production becomes insignificant (table 3). We therefore assume that the rate calculations based on $[N_2O^{omz}_{mean}] - [N_2O]$, $[N_2O^{omz}_{max}] - [N_2O]$ and $[N_2O^{omz}_{min}] - [N_2O]$ (cf. §2*c* for details) represent reasonable lower and upper boundaries.

3. RESULTS AND DISCUSSION

(a) *Concentration and rate estimates*

N_2OPR varies between 0 and 3.3 nmol kg^{-1} yr^{-1} with an overall mean N_2OPR of 0.2 ± 0.04 nmol kg^{-1} yr^{-1} (1σ). Between 100 and 500 m depth, N_2OPR averages 0.4 ± 0.04 nmol kg^{-1} yr^{-1} (1σ), whereas below 500 m N_2OPR averages 0.09 ± 0.01 nmol kg^{-1} yr^{-1} (1σ), indicating that the largest concentration of subsurface N_2O is produced in the upper 500 m of the water column. The estimates of the two parametrizations differ only in the second significant figure.

The global distribution of predicted $[N_2O]$ varies between 4 and 31 nmol kg^{-1} and, where measurement data exist, is qualitatively very similar to the measured $[N_2O]$ of our database. Figure 4 shows a comparison of measured and predicted $[N_2O]$ along 110°W. In the oligotrophic part, the predicted concentrations agree quite well with the measured N_2O; in the suboxic zone, the predicted $[N_2O]$ clearly underestimates $[N_2O]$. This could be due to the use of annual mean dissolved $[O_2]$, which might not adequately reflect the location and extent of the oxygen minimum zone at the time of the data acquisition. Our parametrization does not account for the export of $[N_2O]_{xs}$ from highly productive regions, which might also be a reason for the underestimation shown in figure 4. Qualitative patterns are represented very well by our prediction.

Figure 5 shows the estimated $[N_2O]$ distribution in 200 m depth. Concentrations exceeding 40 nmol kg^{-1}, which are only found in the Arabian Sea, are masked out in figure 5 so as not to obscure the overall qualitative patterns. The eastern boundary upwelling systems are clearly displayed. Concentrations in the Antarctic are slightly elevated, owing to the cold temperatures increasing solubility and thus elevated $[N_2O]_{eq}$. Highest concentrations, 90 nmol kg^{-1}, occur in the Arabian Sea. Concentrations are also comparatively high in the North Pacific Ocean and the Bay of Bengal. Considering the parametrization was solely derived from North Atlantic data, the systematic features of $[N_2O]$ in the world ocean are remarkably well displayed.

Table 3. Constituents of the annual production of nitrous oxide (N_2O) below the mixed layer in Gmol N_2O yr^{-1}. The annual subsurface N_2O yield in Tg N yr^{-1} is given in parentheses.

parameter	depth	temperature
N_2OPR	101.6 ± 24.4	113.2 ± 24.9
N_2OPR^{denit}	6.9 ± 6.9	6.8 ± 6.8
N_2OCR^{denit}	$<0.1 \pm <0.1$	$<0.1 \pm <0.1$
N_2OPR^{arctic}	1.2 ± 0.3	1.3 ± 0.3
N_2OPR_{shelf}	0.5 ± 0.2	0.5 ± 0.2
sum	110.1 ± 31.8	121.7 ± 32.2
	(3.1 ± 0.9)	(3.4 ± 0.9)

$[N_2O]$ is almost always exclusively determined by production via nitrification and $[N_2O]_{eq}$, with the exception of the three oxygen minimum zones. In the oxygen minimum zone in the Arabian Sea, the fraction of N_2O produced via denitrification varies between 2 per cent and 89 per cent between 200 and 900 m. In the oxygen minimum zone of the Eastern Tropical North Pacific, the average fraction of N_2O produced via denitrification per depth varies between 2 per cent and 35 per cent between 400 and 500 m. In the oxygen minimum zone of the Eastern Tropical South Pacific, the average fraction of N_2O produced via denitrification per depth varies between 1 per cent and 14 per cent between 150 and 400 m.

It is worth noting that the qualitative features of $[N_2O]$ are controlled not only by the qualitative features of N_2OPR but also by temperature (via solubility). $[N_2O]_{eq}$ shows patterns very similar to those displayed by $[N_2O]$. We find that $[N_2O]_{eq}$ is strongly controlled by temperature. However, the qualitative features of N_2OPR mainly reflect AOU/*t* and not temperature.

(b) *Annual subsurface nitrous oxide yield*

The integrated annual N_2O production per square metre owing to nitrification is shown in figure 5 and listed in table 3. The qualitative features are similar for both parametrizations. N_2OPR_{temp} estimates a slightly bigger N_2O yield but both parametrizations agree within the error margins. The error analysis suggests that N_2OPR_{temp} estimates the production slightly more accurately (cf. §2*f*; table 2).

The largest amount of N_2O per square metre and per year is produced in the North Atlantic Ocean and off Argentina, which is more likely due to a potential data mismatch between the CFC12- and AOU-datasets in the deep rather than to truly elevated production. Profile data from the North Atlantic [35] suggest there is no significant N_2O production this deep. However, assuming even that true North Atlantic subsurface production amounts only to half of what is predicted by our method would change the global production estimate only by approximately 5 per cent. Production is also very high in the upwelling

regions off Mauritania and Chile, and is elevated in the North Pacific Ocean, the Southern Ocean and parts of the Indian Ocean. However, even if the N_2O yield per square metre is relatively high in the Southern Ocean, then its overall contribution to the global annual production of N_2O is small owing to the small area covered. Overall, the patterns of N_2OPR in the deep ocean—and therefore, the patterns in the mean age in our case—govern the N_2O yield of the water column. Larger water depth does, however, also lead to a larger N_2O yield per square metre without N_2OPR being significantly higher for the involved grid cells.

It should be noted that areas of extensive subsurface production must not necessarily coincide with areas of large sea-to-air fluxes because of the effects of advection. In addition, the yield per square metre does not necessarily illustrate the respective contribution of the different oceanic regions to the overall N_2O source very well, as a high yield per square metre does not necessarily equal a large regional contribution, depending on the area of the respective region.

As denitrification is relevant only in suboxic environments, it has an impact only on the N_2O yield of the suboxic zones in the Arabian Sea and in the Eastern Tropical Pacific. The production yield via denitrification is badly constrained (cf. table 3) and probably also highly variable, but—despite the locally limited influence of denitrification—it yields on average approximately 7 per cent of the total amount of N_2O produced via nitrification (cf. table 3). However, these results are to be viewed with caution as the estimation of N_2OPR^{denit} inherently depends on the predicted N_2OPR. Nevertheless, our estimate is considerably lower than previous estimates of the global contribution of denitrification that range from 25 to 50 per cent [7,9].

Shelf areas account only for less than 0.5 per cent of the subsurface production of N_2O (table 3). This is in line with the conclusions of Bange [36] and Barnes & Upstill-Goddard [37], who suggested that N_2O production in coastal areas, which are not affected by upwelling, is found only in estuaries and river plumes but not on the open shelf. A large fraction of estuarine N_2O comes from sedimentary sources (most probably denitrification). N_2O production from estuaries is, therefore, an additional source of N_2O; however, this is not taken into account in this study.

The overall global annual subsurface production of N_2O amounts to 3.1 ± 0.9 Tg N yr^{-1} (110.1 ± 31.8 Gmol N_2O yr^{-1}) and 3.4 ± 0.9 Tg N yr^{-1} (121.7 ± 32.2 Gmol N_2O yr^{-1}), respectively, and is detailed in table 3. Our N_2O production estimate is in good agreement with the estimate of 3.9 Tg N yr^{-1} by Suntharalingam & Sarmiento [38], but it is lower than the estimate of 5.8 ± 2 Tg N yr^{-1} by Nevison *et al.* [33].

Recent estimates based on gas-exchange parametrizations, compiled by Bange [4], estimate an oceanic source between 1.4 and 14 Tg N yr^{-1} with a mean oceanic source of 6.6 ± 3.6 Tg N yr^{-1} (1σ) based on gas-exchange parametrization, surface measurements and models. Rhee *et al.* [39] recently estimated global N_2O emissions of 0.9–1.7 Tg N yr^{-1} based on extrapolation of measurements in the open Atlantic Ocean. The annual production of N_2O in the ocean is obviously an upper boundary for the annual ocean atmosphere flux. Our production estimate is in agreement with the global emission estimates, especially in view of the uncertainties associated with the emission estimates.

4. SUMMARY

- The predicted N_2O production rates owing to nitrification according to both our suggested parametrizations, N_2OPR_{temp} and N_2OPR_{depth}, show the same qualitative features. However, overall N_2OPR_{temp} estimates slightly higher production than N_2OPR_{depth}. N_2OPR in the deep ocean is comparatively uniform. The largest amount of subsurface N_2O is produced in the upper 500 m of the water column.
- The predicted [N_2O] is qualitatively very similar to measured [N_2O]. Concentrations in the Antarctic Ocean are slightly elevated, whereas highest concentrations occur in the northeastern Pacific Ocean. Temperature is an important control of qualitative features of [N_2O] due to its effect on solubility.
- Our estimates of N_2O production via denitrification are badly constrained, but despite its locally limited influence, the production yield via denitrification on average amounts to approximately 7 per cent of the total amount of N_2O produced via nitrification.
- Shelf areas may account for only less than 0.5 per cent of the global production of oceanic N_2O; however, potential coastal sources of N_2O from estuaries and upwelling areas are not taken into account in our study.
- The annual subsurface N_2O yield amounts to between 3.1 ± 0.9 (N_2OPR_{depth}) and 3.4 ± 0.9 Tg N yr^{-1} (N_2OPR_{temp}), respectively. The annual yield of N_2OPR_{temp} is generally slightly larger than that of N_2OPR_{depth}. The error analysis suggests that N_2OPR_{temp} estimates the production slightly more accurately.
- Our estimate of the total annual N_2O subsurface yield is in agreement with of recent estimates of the global N_2O emissions based on gas-exchange parametrization.

In summary, our findings emphasize that the marine N_2O cycling, production and emissions are still not well understood and still associated with a high degree of uncertainty.

5. OUTLOOK

(a) *Nitrous oxide source in the mixed layer*

Because the mixed layer is well oxygenated, a significant N_2O source in the mixed layer originating from denitrification processes seems unlikely. Until recently, nitrification was thought to be inhibited by light [40]—making it a very unlikely occurrence in the mixed layer. The results of Bange [41], who concluded that the surface layer N_2O concentration in the Arabian Sea is mainly controlled by gas exchange, entrainment of N_2O from deeper layers and variability in the sea surface temperature, are in line with this. It should be noted, however, that assuming a uniform mixed layer

depth of 50 m and a ventilation time of N_2O of three weeks [42], a mixed layer source of 1 Tg N yr^{-1} would lead only to an accumulation of approximately 0.09 nmol kg^{-1} in the mixed layer. Assuming a uniform mixed layer depth of 20 m and a mixed layer source of 1 Tg N yr^{-1} would lead only to an accumulation of approximately 0.2 nmol kg^{-1} in the mixed layer. These changes could probably not be distinguished from natural variability in the surface, even if the method's precision allowed for their detection.

Model results by Yool *et al.* [43], based on nitrification measurements, suggest something very different. They suggest a significant nitrification activity in the euphotic zone. Clark *et al.* [44] measured NH_4^+ and NO_2^- oxidation rates on a north–south transect through the Atlantic Ocean. Their data suggest that in the oligotrophic Atlantic Ocean there is nitrification in the photic zone, which is of sufficient intensity to turn over the NO_3^--pool in one day. Wankel *et al.* [45] found that 17–25% of the nitrate-based productivity in the euphotic zone of Monterey Bay is supported by nitrification. Bianchi *et al.* [46] measured significant nitrification rates in the upper 100 m of the Indian sector of the Southern Ocean. The results of the studies introduced above indicate that there might be indeed significant nitrification activity in the euphotic zone on a global scale. However, there only a few studies that deal with the associated N_2O yield by nitrification in the mixed layer: Dore and Karl [47] used *in situ* measurements of [N_2O] at the ALOHA (A Long-Term Oligotrophic Habitat Assessment) station and the gas-exchange model of Wanninkhof [48] to calculate N_2O ocean–atmosphere fluxes. They calculated the flux to the euphotic zone using concentration gradients and an eddy-diffusivity coefficient of 3.7×10^{-5} m^2 s^{-1}. They used these flux estimates to calculate a net N_2O production rate in the euphotic zone of 1.68–7.94 μmol m^{-2} d^{-1}, which they attribute to *in situ* nitrification. Assuming a N_2O yield of 0.5 per cent during nitrification, nitrification estimates derived from the N_2O production rate were on the same order of magnitude as their directly measured nitrification rates. Even taking into account the probably rather large uncertainties involved in all the calculations, these results clearly point towards a significant N_2O production via nitrification in the euphotic zone. Slightly larger (super-) saturations of N_2O in the upper 40 m of the water column might even have suggested near-surface production. Morell *et al.* [49], Charpentier *et al.* [50] and Law & Ling [51] calculated the air–sea N_2O flux based on their data from the Atlantic Ocean/Caribbean Sea, the central and eastern South Pacific Ocean and the Australasian sector of the Southern Ocean, respectively. They also found a difference between cross-thermocline and air–sea N_2O fluxes in the range of Dore & Karl [47]. They acknowledge that this difference might possibly be due to nitrification [49,51], as indicated by experimental evidence of Dore & Karl [47] and Dore *et al.* [52], or suggested a further hitherto unknown production process [50]. We found the cross-thermocline flux of N_2O in the North Atlantic Ocean calculated from *in situ* N_2O data to be an order of magnitude smaller than the N_2O flux across the air–sea interface calculated using gas-exchange parametrizations [53].

While these results presented above seem to point towards a significant N_2O production via nitrification in the euphotic zone, the probably rather large uncertainties involved in all these calculations need to be taken into account [51,54]. Air–sea fluxes are usually estimated using empirical air–sea gas-exchange parametrizations, which introduces large uncertainties into source estimates. A suite of rather different parametrizations exists, which all fit some experimental dataset, showing that gas exchange itself is highly variable and the governing mechanisms are not yet fully understood [55]: a recent study of both the N_2O air–sea fluxes and the N_2O diapycnal fluxes into the mixed layer revealed that, by using a common gas-exchange approach, the mean air–sea flux is about four times larger than the mean diapycnal flux into the mixed layer. Vertical advection or biological production was found not sufficient to compensate this discrepancy. Instead, flux calculations using an air–sea exchange parametrization that takes into account the effect of surfactants in the ocean surface microlayer are in good agreement with the diapycnal fluxes, indicating that surfactants, especially in areas with a high biological productivity, may have a large dampening effect on air–sea gas exchange of N_2O [54].

There is, however, also an inherent problem with using any kind of gas-exchange model involving the air–sea gradient of some species to estimate long-term average fluxes. Commonly used gas-exchange parametrizations are a measure of an instant sea-to-air flux. After the transfer of molecules, the concentration gradient between the surface water and the atmosphere changes, changing the gas transfer in turn. While this is of no/little consequence to the instant/short-term flux across the air–sea interface, it becomes important when an instant gas-exchange flux is extrapolated over time. Lacking a term to account for the change in concentration over time, it is implicitly assumed in this kind of calculation that any amount of gas lost to the atmosphere from surface waters is instantly replaced from below. In addition, flux estimates based on gas-exchange calculations could be distinctly overestimated as they fail to take the annual cycle of the N_2O flux across the air–sea interface into account [53]. Such an overestimation is even more likely as the underlying datasets are mostly seasonally biased. Both these effects can result in an overestimation of the sea-to-air flux, partly explaining the slight discrepancy we encountered here. Additionally, considering the nonlinear dependence on wind speed of almost all gas-exchange parametrizations, it is at least questionable if the use of averaged wind speeds results in a reasonable estimate of the average air–sea flux.

(b) *Nitrous oxide and deoxygenation of the ocean*

Stramma *et al.* [23] showed that the oxygen minimum zones of the intermediate layers (300–700 m water depth) in various regions of the ocean are expanding and have been losing oxygen during the past 50 years. This would result in an expansion of the zones

supporting denitrification, which would probably have an impact on the production and decomposition of N_2O. Whether it would have a net positive or net negative effect on N_2O production remains unclear as the net behaviour of denitrification and its controlling mechanisms are not yet fully understood [21]. As N_2O yields during both bacterial and archaeal nitrification have been found to be enhanced under low oxygen conditions in laboratory studies [56,57], this increase in volume will probably also lead to increased production of N_2O owing to nitrification. Please note that Frame and Casciotti [58] recently showed that the bacterial N_2O production via nitrification seems to be less sensitive to $[O_2]$ than previously thought [56]. This is in line with the results of two recent studies by Löscher *et al.* [57] and Santoro *et al.* [59] which indicate that oceanic N_2O production is dominated by archaeal nitrification which, in turn, showed a considerably stronger $[O_2]$ sensitivity in culture experiments [57].

(c) *Nitrous oxide from anammox*

The traditional view that denitrification is the dominant process in suboxic oxygen minimum zone has been challenged by the finding that in the oxygen minimum zone of the Eastern Tropical South Pacific and off Namibia the N_2 loss might be almost exclusively performed by bacterial anammox (i.e. anaerobic ammonia oxidation: $NO_2^- + NH_4^+ \rightarrow N_2$) [60,61]. However, so far, N_2O has only been found to be produced during anammox in relatively small quantities during nitric oxide detoxification ($NO_2^- \rightarrow NO \rightarrow N_2O$), which seems to be performed by the anammox bacterium *Kuenenia stuttgartiensis* as a side reaction [62]. Thus, the role of marine anammox bacteria in N_2O cycling in suboxic oxygen minimum zones remains to be verified.

(d) *Nitrous oxide from coastal hypoxia*

Estuaries and nitrogen rich coastal zones probably contribute to a significant degree to the total oceanic emissions of N_2O [63,64]. Estuaries and their adjacent regions are fertilized to an increasing degree by river run-off carrying a high load of organic nitrogen. This fertilization may lead to enhanced primary production and thus enhanced nitrification and N_2O formation in an increasing number of $[O_2]$ depleted (i.e. hypoxic) coastal areas [65]. Additionally, the changing flux of organic material reaching the sediments might change O_2 concentrations in the sediment, changing N_2O production in turn. And, unlike in the open ocean, the shallow depths of coastal regions allow for N_2O produced in the sediments to reach the atmosphere.

(e) *Warming of the ocean*

There is evidence that the oceans are warming [66,67]. As marine autotrophic and heterotrophic processes display sensitivities to temperature (to varying degrees), ocean warming might result in changes of the bacterial community structure and hence in changes of N_2O production. Changes in ocean temperature also affect the solubility of N_2O. Rising ocean temperature implies that the N_2O long-term storage capacity of the deep ocean will be reduced. Additionally, this effect will temporarily strengthen the N_2O source, as apparent supersaturations created by warming water masses after their last contact with the atmosphere will increase the ocean–atmosphere gradient when these water masses finally get into contact with the atmosphere again. This strengthening effect will disappear again once the temperature change levels off and the system reaches equilibrium again. In addition, non-uniform warming could induce enhanced stratification of the water column. This could potentially diminish the oceanic N_2O source by keeping N_2O-rich water from intermediate depths from reaching the air–sea interface.

(f) *Ocean acidification*

The ongoing increase of CO_2 in the atmosphere also causes a decrease of the oceanic pH (i.e. ocean acidification). This, in turn, results in a shift of the NH_3–NH_4^+ equilibrium towards NH_4^+. In a recent study by Beman *et al.* [68], it was shown that nitrification rates decreased significantly when the pH was lowered to values expected to occur in the future ocean. (One explanation for the pH sensitivity of nitrification rates is that the ammonia monooxygenase enzyme uses NH_3 rather than NH_4^+ as substrate in the first step of the nitrification sequence [69].) On the basis of these results, it was suggested by Beman *et al.* [68] that future oceanic N_2O production during nitrification should be decreased as well. However, this scenario might be not that straightforward: nitrification is part of organic matter remineralization (i.e. oxidation of organic matter with O_2 to CO_2). Therefore, both pH and O_2 are decreasing during organic matter remineralization. However, it is well known that decreasing O_2 concentrations lead to increasing N_2O production during nitrification [57] and obviously there seems to be only a minor effect of decreasing pH on N_2O production during nitrification as part of the organic matter remineralization process. Laboratory experiments to verify the effect of ocean acidification on N_2O production via nitrification are missing.

H.W.B. is grateful for the invitation to the Theo Murphy Meeting 'Nitrous oxide: the forgotten greenhouse gas' at the Kavli Royal Society International Centre, 23–24 May 2011. We thank two anonymous reviewers for their constructive comments. The authors are indebted to each of the individual contributors who generously submitted their data to the marine methane and nitrous oxide database (MEMENTO). We thank Toste Tanhua for helpful discussions about the TTD method. This study was supported by the German Science Foundation (DFG) by research grants no. DFG BA1990/7 and BMBF grant no. 03F0462A (SOPRAN).

REFERENCES

1 IPCC 2007 *Climate change 2007: the physical science basis. Contribution of working group I to the fourth assessment report of the intergovernmental panel on climate change* (eds S. Solomon, D. Qin, M. Manning, Z. Chen, M. Marquis, K. B. Averyt, M. Tignor, H. L. Miller), p. 996. Cambridge, UK: Cambridge University Press.
2 WMO 2011 Scientific assessment of ozone depletion: 2010, global ozone research and monitoring project. Report no. 52. Geneva, Switzerland: WMO.
3 Forster, P. *et al.* 2007 Changes in atmospheric constituents and in radiative forcing. In *Climate change 2007: the physical science basis. Contribution of working group I*

to the fourth assessment report of the intergovernmental panel on climate change (eds S. Solomon, D. Qin, M. Manning, Z. Chen, M. Marquis, K. B. Averyt, M. Tignor & H. L. Miller), pp. 129–234. Cambridge, UK: Cambridge University Press.

4 Bange, H. W. 2006 New directions: the importance of the oceanic nitrous oxide emissions. *Atmos. Environ.* **40**, 198–199. (doi:10.1016/j.atmosenv.2005.09.030)

5 Denman, K. L. *et al.* 2007 Couplings between changes in the climate system and biogeochemistry. In *Climate change 2007: the physical science basis. Contribution of working group I to the fourth assessment report of the intergovernmental panel on climate change* (eds S. Solomon, D. Qin, M. Manning, Z. Chen, M. Marquis, K. B. Averyt, M. Tignor & H. L. Miller), pp. 499–587. Cambridge, UK: Cambridge University Press.

6 Bange, H. W., Freing, A., Kock, A. & Löscher, C. R. 2010 Marine pathways to nitrous oxide. In *Nitrous oxide and climate change* (ed. K. Smith), pp. 36–62. London, UK: Earthscan.

7 Bange, H. W. & Andreae, M. O. 1999 Nitrous oxide in the deep waters of the world's oceans. *Glob. Biogeochem. Cycles* **13**, 1127–1135. (doi:10.1029/1999GB900082)

8 Codispoti, L. A. 2010 Interesting times for marine N_2O. *Science* **327**, 1339–1340. (doi:10.1126/science.1184945)

9 Suntharalingam, P., Sarmiento, J. L. & Toggweiler, J. R. 2000 Global significance of nitrous oxide production and transport from oceanic low-oxygen zones: a modeling study. *Glob. Biogeochem. Cycles* **14**, 1353–1370. (doi:10.1029/1999GB900100)

10 Freing, A., Wallace, D. W. R., Tanhua, T., Walter, S. & Bange, H. W. 2009 North Atlantic production of nitrous oxide in the context of changing atmospheric levels. *Glob. Biogeochem. Cycles* **23**, GB4015. (doi:10.1029/2009GB003472)

11 Locarnini, R. A., Mishonov, A. V., Antonov, J. I., Boyer, T. P. & Garcia, H. E. 2006 *World Ocean Atlas 2005, Volume 1: Temperature* (ed. S. Levitus). Washington, DC: NOAA.

12 Antonov, J. I., Locarnini, R. A., Boyer, T. P., Mishonov, A. V. & Garcia, H. E. 2006 *World Ocean Atlas 2005, Volume 2: Salinity* (ed. S. Levitus). Washington, DC: NOAA.

13 Garcia, H. E., Locarnini, R. A., Boyer, P. & Antonov, J. I. 2006 *World Ocean Atlas 2005, Volume 3: Dissolved oxygen, apparent oxygen utilization and oxygen saturation* (ed. S. Levitus). Washington, DC: NOAA.

14 Key, R. M. *et al.* 2004 A global ocean carbon climatology: results from Global Data Analysis Project (GLODAP). *Glob. Biogeochem. Cycles* **18**, GB4031. (doi:10.1029/2004GB002247)

15 Matsumoto, K. 2007 Radiocarbon-based circulation of the world oceans. *J. Geophys. Res.* **112**, C09004. (doi:10.1029/2007JC004095)

16 Machida, T., Nakazawa, T., Fujii, Y., Aoki, S. & Watanabe, O. 1995 Increase in the atmospheric nitrous oxide concentration during the last 250 years. *Geophys. Res. Lett.* **22**, 2921–2924. (doi:10.1029/95GL02822)

17 Battle, M. *et al.* 1996 Atmospheric gas concentrations over the past century measured in air from firn at the South Pole. *Nature* **383**, 231–235. (doi:10.1038/383231a0)

18 Holland, E. A., Lee-Taylor, J., Nevison, C. & Sulzman, J. 2005 Fluxes and N_2O mixing ratios originating from human activity. See http://www.daac.ornl.gov.

19 de Boyer Montégut, C., Madec, G., Fischer, A. S., Lazar, A. & Iudicone, D. 2004 Mixed layer depth over the global ocean: an examination of profile data and a profile-based climatology. *J. Geophys. Res.* **109**, C12003. (doi:10.1029/2004JC002378)

20 Bange, H. W., Bell, T. G., Cornejo, M., Freing, A., Uher, G., Upstill-Goddard, R. C. & Zhang, G. 2009 MEMENTO: a proposal to develop a database of marine nitrous oxide and methane measurements. *Environ. Chem.* **6**, 195–197. (doi:10.1071/EN09033)

21 Devol, A. H. 2008 Denitrification including anammox. In *Nitrogen in the marine environment*, 2nd edn. (eds D. G. Capone, D. A. Bronk, M. R. Mulholland & E. J. Carpenter), pp. 263–301. Amsterdam, The Netherlands: Elsevier.

22 Codispoti, L. A., Elkins, J. W., Yoshinari, T., Friederich, G. E., Sakamoto, C. M. & Packard, T. T. 1992 On the nitrous oxide flux from productive regions that contain low oxygen waters. In *Oceanography of the Indian Ocean* (ed. B. N. Desai), pp. 271–284. Rotterdam, The Netherlands: A.A. Balkema.

23 Stramma, L., Johnson, G. C., Sprintall, J. & Mohrholz, V. 2008 Expanding oxygen minimum zones in the tropical oceans. *Science* **320**, 655–658. (doi:10.1126/science.1153847)

24 Paulmier, A. & Ruiz-Pinto, D. 2009 Oxygen minimum zones in the modern ocean. *Prog. Oceanogr.* **80**, 113–128. (doi:10.1016/j.pocean.2008.08.001)

25 Naqvi, S. W. A. & Shailaja, M. S. 1993 Activity of the respiratory electron transport system and respiration rates within the oxygen minimum layer of the Arabian Sea. *Deep-Sea Res. Part II* **40**, 687–695. (doi:10.1016/0967-0645(93)90052-O)

26 Olson, D. B., Hitchcock, G. L., Fine, R. A. & Warren, B. A. 1993 Maintenance of the low-oxygen layer in the central Arabian Sea. *Deep-Sea Res. Part II* **40**, 673–685. (doi:10.1016/0967-0645(93)90051-N)

27 Karstensen, J., Stramma, L. & Visbeck, M. 2008 The oxygen minimum zones in the eastern tropical Atlantic and Pacific Oceans. *Prog. Oceanogr.* **77**, 331–350. (doi:10.1016/j.pocean.2007.05.009)

28 Feely, R. A., Sabine, C. L., Schlitzer, R., Bullister, J. L., Mecking, S. & Greeley, D. 2004 Oxygen utilization and organic carbon remineralization in the upper water column of the Pacific Ocean. *J. Oceanogr.* **60**, 45–52. (doi:10.1023/B:JOCE.0000038317.01279.aa)

29 Jenkins, W. J. & Wallace, D. W. R. 1992 Tracer based inferences of new primary production in the sea. In *Primary productivity and biogeochemical cycles* (eds P. G. Falkowski & A. D. Woodhead), pp. 299–316. New York, NY: Plenum Press.

30 Tanhua, T., Körtzinger, A., Friis, K., Waugh, D. W. & Wallace, D. W. R. 2007 An estimate of anthropogenic CO_2 inventory from decadal changes in oceanic carbon content. *Proc. Natl Acad. Sci. USA* **104**, 3037–3042. (doi:10.1073/pnas.0606574104)

31 England, M. H. 1995 The age of water and ventilation timescales in a global ocean model. *J. Phys. Oceanogr.* **25**, 2756–2777. (doi:10.1175/1520-0485(1995)025<2756:TAOWAV>2.0.CO;2)

32 Peacock, S. & Maltrud, M. 2006 Transit-time distributions in a global model. *J. Phys. Oceanogr.* **36**, 474–495. (doi:10.1175/JPO2860.1)

33 Nevison, C., Butler, J. H. & Elkins, J. W. 2003 Global distribution of N_2O and ΔN_2O–AOU yield in the subsurface ocean. *Glob. Biogeochem. Cycles* **17**, 1119. (doi:10.029/2003GB002068)

34 Farías, L., Paulmier, A. & Gallegos, M. 2007 Nitrous oxide and N-nutrient cycling in the oxygen minimum zone off northern Chile. *Deep-Sea Res. Part I* **54**, 164–180. (doi:10.1016/j.dsr.2006.11.003)

35 Walter, S., Bange, H. W., Breitenbach, U. & Wallace, D. W. R. 2006 Nitrous oxide in the North Atlantic Ocean. *Biogeosciences* **3**, 607–619. (doi:10.5194/bg-3-607-2006)

36 Bange, H. W. 2006 Nitrous oxide and methane in European coastal waters. *Estuar. Coastal Shelf Sci.* **70**, 361–374. (doi:10.1016/j.ecss.2006.05.042)

37 Barnes, J. & Upstill-Goddard, R. C. 2011 N_2O seasonal distribution and air–sea exchange in UK estuaries:

implications for tropospheric N_2O source from European coastal waters. *J. Geophys. Res.* **116**, G01006. (doi:10.1029/2009JG001156)
38 Suntharalingam, P. & Sarmiento, J. L. 2000 Factors governing the oceanic nitrous oxide distribution: simulations with an ocean general circulation model. *Glob. Biogeochem. Cycles* **14**, 429–454. (doi:10.1029/1999GB900032)
39 Rhee, T. S., Kettle, A. J. & Andreae, M. O. 2009 Methane and nitrous oxide emissions from the ocean: a reassessment using basin-wide observations in the Atlantic. *J. Geophys. Res.* **114**, D12304. (doi:10.1029/2008JD011662)
40 Horrigan, S. G., Carlucci, A. F. & Williams, P. M. 1981 Light inhibition of nitrification in sea-surface films. *J. Mar. Res.* **39**, 557–565.
41 Bange, H. W. 2004 Air–sea exchange of nitrous oxide and methane in the Arabian Sea: a simple model of the seasonal variability. *Indian J. Mar. Sci.* **33**, 77–83.
42 Najjar, R. G. 1992 Marine biogeochemistry. In *Climate system modeling* (ed. K. E. Trenberth), pp. 241–280. Cambridge, UK: Cambridge University Press.
43 Yool, A., Martin, A. P., Fernández, C. & Clark, D. R. 2007 The significance of nitrification for oceanic new production. *Nature* **447**, 999–1002. (doi:10.1038/nature05885)
44 Clark, D. R., Rees, A. P. & Joint, I. 2008 Ammonium regeneration and nitrification rates in the oligotrophic Atlantic Ocean: implications for new production estimates. *Limnol. Oceanogr.* **53**, 52–62. (doi:10.4319/lo.2008.53.1.0052)
45 Wankel, S. D., Kendall, C., Pennington, J. T., Chavez, F. P. & Paytan, A. 2007 Nitrification in the euphotic zone as evidenced by nitrate isotopic composition: observation from Monterey Bay, California. *Glob. Biogeochem. Cycles* **21**, GB2009. (doi:10.1029/2006GB002723)
46 Bianchi, M., Feliatra, F., Treguer, P., Vincendeau, M.-A. & Morvan, J. 1997 Nitrification rates, ammonium and nitrate distribution in upper layers of the water column and in sediments of the Indian sector of the Southern Ocean. *Deep-Sea Res. Part II* **44**, 1017–1032. (doi:10.1016/S0967-0645(96)00109-9)
47 Dore, J. E. & Karl, D. M. 1996 Nitrification in the euphotic zone as a source for nitrite, nitrate, and nitrous oxide at station ALOHA. *Limnol. Oceanogr.* **41**, 1619–1628. (doi:10.4319/lo.1996.41.8.1619)
48 Wanninkhof, R. 1992 Relationship between wind speed and gas exchange over the ocean. *J. Geophys. Res.* **97**, 7373–7382. (doi:10.1029/92JC00188)
49 Morell, J. M., Capella, J., Mercado, A., Bauzá, J. & Corredor, J. E. 2001 Nitrous oxide fluxes in Caribbean and tropical Atlantic waters: evidence for near surface production. *Mar. Chem.* **74**, 131–143. (doi:10.1016/S0304-4203(01)00011-1)
50 Charpentier, J., Farias, L. & Pizarro, O. 2010 Nitrous oxide fluxes in the central and eastern South Pacific. *Glob. Biogeochem. Cycles* **24**, GB3011. (doi:10.1029/2008GB003388)
51 Law, C. S. & Ling, R. D. 2001 Nitrous oxide flux and response to increased iron availability in the Antarctic Circumpolar Current. *Deep-Sea Res. Part II* **48**, 2509–2527. (doi:10.1016/S0967-0645(01)00006-6)
52 Dore, J. E., Popp, B. N., Karl, D. M. & Sansone, F. J. 1998 A large source of atmospheric nitrous oxide from subtropical North Pacific surface waters. *Nature* **396**, 63–66. (doi:10.1038/23921)
53 Freing, A. 2009 Production and emissions of oceanic nitrous oxide. PhD thesis, University of Kiel, Kiel, Germany.
54 Kock, A., Schafstall, J., Brandt, P., Dengler, M. & Bange, H. W. 2011 Air–sea and diapycnal nitrous oxide fluxes in the eastern tropical North Atlantic Ocean. *Biogeosci. Dis.* **8**, 10 229–10 246.
55 Wanninkhof, R., Asher, W. E., Ho, D. T., Sweeney, C. & McGillis, W. R. 2009 Advances in quantifying air–sea gas exchange and environmental forcing. *Annu. Rev. Mar. Sci.* **1**, 213–244. (doi:10.1146/annurev.marine.010908.163742)
56 Goreau, T. J., Kaplan, W. A., Wofsy, S. C., McElroy, M. B., Valois, F. W. & Watson, S. W. 1980 Production of NO_2^- and N_2O by nitrifying bacteria at reduced concentrations of oxygen. *Appl. Environ. Microbiol.* **40**, 526–532.
57 Löscher, C., Kock, A., Könneke, M., LaRoche, J., Bange, H. W. & Schmitz, R. Submitted. Ammonia-oxidizing archaea dominate oceanic nitrous oxide production in the OMZ off Mauritania. *Biogeosciences*.
58 Frame, C. H. & Casciotti, K. L. 2010 Biogeochemical controls and isotope signatures of nitrous oxide production by a marine ammonia-oxidizing bacterium. *Biogeosciences* **7**, 2695–2709. (doi:10.5194/bg-7-2695-2010)
59 Santoro, A. E., Buchwald, C., McIlvin, M. R. & Casciotti, K. L. 2011 Isotopic signature of N_2O produced by marine ammonia-oxidizing archaea. *Science* **333**, 1282–1285. (doi:10.1126/science.1208239)
60 Lam, P. *et al.* 2009 Revising the nitrogen cycle in the Peruvian oxygen minimum zone. *Proc. Natl Acad. Sci. USA* **106**, 4752–4757. (doi:10.1073/pnas.0812444106)
61 Kuypers, M. M. M., Lavik, G., Woebken, D., Schmid, M., Fuchs, B. M., Amann, R., Jørgensen, B. B. & Jetten, M. S. M. 2005 Massive nitrogen loss from Benguela upwelling system through anaerobic ammonium oxidation. *Proc. Natl Acad. Sci. USA* **102**, 6478–6483. (doi:10.1073/pnas.0502088102)
62 Kartal, B., Kuypers, M. M. M., Lavik, G., Schalk, J., Op den Camp, H. J. M., Jetten, M. S. M. & Strous, M. 2007 Anammox bacteria disguised as denitrifiers: nitrate reduction to dinitrogen gas via nitrite and ammonium. *Environ. Microbiol.* **9**, 635–642. (doi:10.1111/j.1462-2920.2006.01183.x)
63 Kroeze, C., Dumont, E. & Seitzinger, S. P. 2005 New estimates of global emissions of N_2O from rivers and estuaries. *Environ. Sci.* **2**, 159–165. (doi:10.1080/15693430500384671)
64 Zhang, G-L., Zhang, J., Liu, S-M., Ren, J-L. & Zhao, Y.-C. 2010 Nitrous oxide in the Changjiang (Yangtze River) estuary and its adjacent marine area: riverine input, sediment release and atmospheric fluxes. *Biogeosciences* **7**, 3505–3516. (doi:10.5194/bg-7-3505-2010)
65 Naqvi, S. W. A., Bange, H. W., Farías, L., Monteiro, P. M. S., Scranton, M. I. & Zhang, J. 2010 Marine hypoxia/anoxia as a source of CH_4 and N_2O. *Biogeosciences* **7**, 2159–2190. (doi:10.5194/bg-7-2159-2010)
66 Barnett, T. P., Pierce, D. W., Achuta Rao, K. M., Gleckler, P. J., Santer, B. D., Gregory, J. M. & Washington, W. M. 2005 Penetration of human induced warming into the world's oceans. *Science* **309**, 284–287. (doi:10.1126/science.1112418)
67 Levitus, S., Antonov, J. I. & Boyer, P. 2005 Warming of the world ocean, 1955–2003. *Geophys. Res. Lett.* **32**, L02604. (doi:10.1029/2004GL021592)
68 Beman, J. M., Chow, C-E., King, A. L., Feng, Y., Fuhrman, J. A., Andersson, A., Bates, N. R., Popp, B. N. & Hutchins, D. A. 2011 Global declines in oceanic nitrification rates as consequence of ocean acidification. *Proc. Natl Acad. Sci. USA* **108**, 208–213. (doi:10.1073/pnas.1011053108)
69 Ward, B. B. 2008 Nitrification in marine systems. In *Nitrogen in the marine environment*, 2nd edn. (eds D. G. Capone, D. A. Bronk, M. R. Mulholland & E. J. Carpenter), pp. 199–261. Amsterdam, The Netherlands: Elsevier.